Version 28/07/2005, submitted to Atmospheric Research

The 6 Hours Climatology of Thunderstorms and Rainfalls in the Friuli Venezia Giulia Plain

Agostino Manzato

agostino.manzato@osmer.fvg.it

Keywords: climatology, thunderstorm, rain, convective, flux.

OSMER – Osservatorio Meteorologico Regionale dell'ARPA Friuli Venezia Giulia

Via Oberdan 18, I–33040 Visco (UD), Italy, tel. +39 0432 934163

Abstract

Friuli Venezia Giulia is a region located in the North–Eastern part of Italy. It has the Adriatic Sea (Gulf of Trieste) on the South and the Julian and Carnic Alps surrounding it on the North. For these geographical properties thunderstorms and precipitations are common events in the plain of this region.

The climatology of thunderstorms and rainfalls, considering 6 h interval periods, is studied in this work. It is shown how the thunderstorm frequency, based on the recording of at least three lightning strikes during the 6 h period, is 16%. The occurrence frequency of at least 1 mm of rain accumulated in 6 h is 24%, while that of at least 5 mm in 6 h is 14%.

The daily and monthly distributions of these events are then stratified in three classes, based on their "intensity" (weak, medium and strong), and the different behaviors are analysed. Finally, an explanation for the main monthly rain frequency is sought by looking at only two sounding–derived indices and in particular at their annual cycles. The two indices (related to the potential instability and to the water vapour flux) attempt to summarize the "convective" and "flux" mechanisms for producing rain. It is found that in some particular periods of the year the rain–originating process seems well identifiable, while in many others the two processes seem to be concomitant.

1 Introduction

The rainfall climatology in Friuli Venezia Giulia (hereafter FVG) has been already studied by different authors. In his copious volume of 1964 prof. Joseph Gentilli (Univ. of Western Australia) analysed all the different aspects of FVG climate, including thunderstorms and rainfalls, based on the historical information available 40 years ago (Gentilli, 1964). Ceschia et al. (1991) studied the 1951–1986 database of monthly precipitations, dividing the FVG plain in two climatologically different parts: "coastal" and "plain". Cicogna et al. (2000) studied the 1991–1997 hourly rainfall data measured by the OSMER–ARPA meteorological network, refining the FVG plain division into five climatologically homogeneous areas.

Manzato (2003) described the thunderstorm climatology in the FVG plain, based on 6 h periods, using the 1995–2001 database of cloud–to–ground (hereafter C2G) lightning strikes and the hourly data measured by the OSMER–ARPA meteorological network. This work was based on 6 h periods, because the Udine sounding is performed every 6 h and the thunderstorm occurrence and intensity were studied relative to the sounding–derived instability indices. The climatology of FVG lightnings has been partially covered also by Schulz et al. (2005). In their work it is possible to see how the lightning frequency is much larger in FVG with respect to Austria and Slovenia.

Lastly, for its high frequency of heavy rain, the FVG region was included as one of the target areas during the Intense Observing Periods (hereafter IOP) of the international "Mesoscale Alpine Project" (see http://www.map.ethz.ch). For this reason, information on FVG rainfall climatology and some case studies can be found also in the MAP literature. For example Frei and Schär (1998) have shown how FVG and West Slovenia is one of the three southern Alpine regions with climatologically most frequent heavy rainfall. Single flood cases (in particular IOP 5 and IOP 2 b) have been studied in detail, for example by Pradier et al. (2001) and Vrhovec et al. (2004).

The next section presents the data used in this work, while sections 3 and 4 will derive from these data the FVG thunderstorm and rainfall climatology. Sections 5 and 6 try to discriminate the rain episodes in two classes, each one associated to a particular sounding–

derived index, and to use the trend of these indices to explain the rain monthly variability.

2 Target area and observation facilities

Figure 1 shows the target area map and orography. It is the plain of Friuli Venezia Giulia (North–East Italy), with an area of about 5.000 km^2. On the North it is bordered by the Alps, while on the South there are the Adriatic Sea and the Grado and Marano lagoons. There is no climatological separation of the target area into sub–regions, but four sub–areas are defined in order to compute the thunderstorm "total rain" (see below).

Inside the target area there are 15 OSMER–ARPA mesonet synoptic stations. 11 out of these 15 surface stations were operative before 1992, 2 began to work during 1992, 1 after March 1993 and 1 after June 1994. These stations automatically record hourly data, while 14 of them also collect 5–minute data, which in this work are used only to look for the wind gust. Actually OSMER–ARPA manages a network of almost 30 synoptical stations, but those placed in the mountains or with less than 10 years of data were not considered.

In the center of the plain there is also the radiosounding station of Udine–Campoformido (WMO code 16044), managed by the Italian Aereonautica Militare. From 1984 to January 2002 the radiosonde used was the Vaisala RS-80, while after the Vaisala RS-90 was used. Since 1986 this station has always done four soundings per day, one every 6 hours. Only from October 2004 to June 2005 the 18 UTC radiosounding has been discontinued and that had some consequences on the OSMER–ARPA operational tools based on 6 h radiosoundings.

Finally, the data of the Italian network for C2G lightning detection, managed by CESI/SIRF (see http://www.fulmini.it for details), have been used for the thunderstorm occurrence and intensity study. The lightning data are available for the FVG region only since 1995.

3 FVG 6 h thunderstorm climatology

The cases analysed for the thunderstorm climatology are all of the 6 h periods with non–missing sounding from 1 April to 30 November of the years 1995–2004. The database contains 9210 different cases. The "active" cases (i.e. thundery: at least three C2G lightnings registered during the 6 h) are 1505, which are 16.3% out of the total. In previous works by the same author the climatological frequency of the FVG thunderstorms was much higher (26%), because the cases with only one or two lightnings were considered active and also because the months of October and November, which have low thunderstorm frequency, were not included.

Figure 2 a shows the frequency of thundery cases during the four periods of the day[1]. The total height of each bar shows the class–relative frequency of thundery cases. The frequency relative to each class (i. e. the "6 h–period of the day" thunderstorm posterior probability) has been used instead of the frequency relative to all the database, because the number of total cases in the four classes can be different. For example, there are more missing soundings at 00 UTC than at 12 UTC.

Figure 3 a shows the distribution of the thunderstorm "intensity", as defined using the variable CALCA6h (Manzato 2003) with a threshold of at least three C2G strikes:

$$CALCA\,6h = \begin{cases} \frac{\frac{1}{8}\cdot\ln(1+num\_light)+\frac{1}{6}\cdot\ln(1+rain)+\frac{1}{3}\cdot\ln(1+wind)}{2.9} & \text{if } num\_light \geq 3, \\ 0 & \text{if } num\_light < 3. \end{cases} \quad (1)$$

CALCA6h is the sum of the normalized natural logarithm of these three activity variables: the number of lightning strikes (*num_light*) which hit the target area during the 6 h; the total rain (*rain*) as the sum of all the four maximum hourly rain values in the four sub–areas (only for the hours with C2G lightning occurrence), and, lastly, the maximum 5–minute wind gust (*wind*) recorded during the 6 h. The CALCA6h distribution of figure 3 a, without the 0 cases, is much more "bell shaped" than that shown in Manzato (2003, figure 2), because there are fewer cases with low intensity. The 10% (0.33) and 90%

[1] These periods start at 5, 11, 17 and 23 UTC, which are the launching time of the 6, 12, 18 and 00 UTC soundings. Note also that local time of Italy is 1 h more than UTC time, or 2 h more during Summer Time.

(0.79) percentiles are marked by a dashed line. The minimum value (0.2) is obtained with three lightning strikes, no rain and very low wind (about 2 m/s). The 2.9 normalization factor assures having a historical maximum of less than 1. The six most intense episodes (CALCA6h > 0.95) are listed in table 1. Note that all these six cases occurred during the evening/nighttime (from 17 to 05 UTC).

The 10% (90%) percentile of CALCA6h is then used to stratify the less (most) intense cases during the four periods of the day. In figure 2 a the light (dark) sector of the frequency bar shows the frequency of the weakest (strongest) cases. It is possible to see how thunderstorms occur most frequently during the afternoon (11–17 UTC), but, if one considers only the strongest cases, the frequency is a maximum during the afternoon and the evening (17–23 UTC). This observation is apparently in disagreement with that of Giaiotti et al. (2001), which shows how the storms producing the *largest hail*[2] in the FVG plain occur during the nighttime (00–06 UTC), followed by the evening and the afternoon periods (work based on a network of about 360 hailpads collected for 15 years). This disagreement can be resolved thinking that large hail is produced not by strong thunderstorms *alone*, but also by other conditions favored mainly during nighttime, such as no solar radiation, lower temperature and higher mixing ratio (as shown in Giaiotti and Stel 2006), which can produce bigger stones and smaller melting effects. The hypothesis that the largest hail producing thunderstorm are not necessarily always the strongest ones was already suggested by Nelson (1983): "... a factor more critical than maximum updraft speed for hail growth is a broad region of moderate updraft (20–40 m/s). This is because in the most severe storms, hail cannot grow in the strongest part of the updraft, but only in the edges [...]. Past a certain threshold, therefore, convective instability is not as important as whatever factors determine the shape of an updraft [...]".

Figure 4 a shows the class–relative frequency of thunderstorm, during the different eight

[2]Large hail in FVG means hail with a diameter of about 2–5 cm. From the Weickmann (1953) equation a 5 cm hailstone can be suspended in an updraft of about 30 m/s, which corresponds to a moderate CAPE (450 J/kg).

months studied. The frequency of all the thunderstorm occurrences, regardless to their intensity, is maximum from June through August. In particular June seems to have a little higher frequency of thunderstorms, as stated also by Buzzi et al. (1991) for the whole Northern Italian basin[3]. On the other hand, if one looks only at the strongest cases, then the maximum frequency appears to be in July and August, while the frequency of the strongest storms in June is much lower and is similar to that of September. Note also how October and November have a frequency of all the thundery cases smaller than that of April, but their frequency of severe thunderstorms is not negligible as is the case in April. Lastly, it is noted how the monthly distribution of all the thundery cases has the same shape as that found by Nappi and Bruno (2004) for the thundery days, as observed from *synop* reports made by the Italian Aereonautica Militare in North–Eastern part of Italy (work based on the 1990–1996 data of five stations with observers).

4 FVG 6 h rain climatology

Another meteorological event studied in this work is the *maximum 6 h rain* measured by any of the 15 OSMER–ARPA stations located in the FVG plain. The cases analysed are all of the 6 h periods, for which the sounding is not missing, of the years 1992–2004. The database contains 17352 cases, and 4147 out of them (23.9%) have a maximum 6 h accumulated rain equal to or higher than 1 mm. The cases with $0 < \mathrm{MaxRain} < 1$ mm in 6 h have been considered as noise and then set as non–occurrences of rain.

Figure 3 b shows the distribution of all the cases with over 1 mm. Since the ordinate scale is logarithmic, the almost linear trend between 10 and 80 mm means a good fit with an exponential distribution. The fitting line in the figure represents the following equation:

$$N \cong 1100\, \mathrm{e}^{-0.075 \cdot MaxRain}\,. \tag{2}$$

Since this distribution is so skewed, instead of using the 10% and 90% percentiles to stratify

[3]In this area Cacciamani et al. (1995) have found a thundery day monthly frequency quite different from that of figure 4 a, i. e. with higher frequency in May and lower frequency in July and August.

the weak/strong precipitations it has been chosen to use the 41% and 95%, which are respectively 5 and 39 mm. Table 2 lists the nine "outliers", i. e. cases with more than 100 mm in 6 h, which can be called flash–flood[4] events. It is interesting to note how six of these nine flash–floods occurred between 12 and 28 September, and also how five of them were measured by four stations which are quite close together[5].

Figure 2 b shows the frequency of rain during the 6 h periods of the day: it is possible to see how there is not so much difference between the four different classes (differently from what was found in the thunderstorm case), even if the maximum frequency still occurs during the afternoon and the evening. More interesting is figure 4 b, which shows the frequency of rain during the different months of the year. Looking at all the precipitation cases it is possible to find two peaks: the first in late Spring (April to June) and the second around October. Instead, looking at only the strongest rainfalls, the maximum occurred in September, followed by October and August. July, August and September have a relatively low frequency of total rain occurrence, but have more heavy precipitation events than Spring or November.

The high frequencies during July and August can be explained by looking at the monthly frequency distribution of the strongest thunderstorms (figure 4 a), which has a maximum in those months. Conversely, the maximum frequency of the strongest cases during September and October can't be explained by convective instability *alone*, but there should be the *concurrence* of some other cause. This cause could be a higher frequency of *Atlantic cold front passages*, which during Summer are usually prevented by a strong anticyclone over the Mediterranean zone. During late September and October there is less instability than in July and August, but probably these thunderstorms are *embedded* in large structures, which can produce more rain and fewer lightning strikes (high MaxRain but not so high

[4] The World Meteorological Organization defines a flash–flood as a short duration inundation with a high peak of flow. Here the term flash–flood means simply "a lot of rain in a short time". All the cases listed in table 2 were associated with some street or field flood, but none of them produced large inundations.

[5] In fact Capriva, Gradisca, Cervignano and Fossalon di Grado can be contained by a rectangle of only 15x30 km, less than 10% of the whole target area.

CALCA6h).

Also during Spring there is a higher frequency of front passages than in Summer, but that does not produce so many strong rainfalls as in Fall. Probably in Spring there is lower relative humidity, because the Sea Surface Temperature (SST) is colder than in Fall. Figure 4 b shows the monthly mean SST measured by the "Trieste Molo" OSMER–ARPA station during the year 1995–2004 (Upper Adriatic line) and the mean SST over the whole Mediterranean Sea during the year 1985–2002, as derived by Marullo and Guarracino (2003) from the NOAA/NASA AVHRR Oceans Pathfinder SST data (for detail see http://podaac.jpl.nasa.gov/sst_doc.html). It is possible to see how the mean SST during April and May is always lower than in September and October. Instead June is more similar to September for the Trieste SST and to October for the mean Mediterranean SST. In any case, June has a lower flux of water vapour (as will be shown in the next section) and a lower mean relative humidity in the lowest 250 hPa of the Udine radiosoundings (figure 6 a) than late September and October.

Lastly, it is very interesting to note how the frequency of cases with more than 39 mm of rainfall correlates better with the mean SST over the entire Mediterranean Sea (R = 0.91, p–value = $4 \cdot 10^{-5}$) than with the Upper Adriatic SST (R = 0.86, p–value = $3 \cdot 10^{-4}$), as if the moist air coming from a large area is needed for the strongest rainfall. In both cases the correlation is statistically significant and better than that with the frequency of cases over 5 mm, which is R = 0.64 (p–value = $2 \cdot 10^{-2}$) for the mean Mediterranean SST and R = 0.74 (p–value = $6 \cdot 10^{-3}$) for the Upper Adriatic SST.

5 A two–index approach to rainfall

OSMER–ARPA forecasters usually try to divide precipitation events in two categories: *convective* and *flux* precipitation. Convective rain is associated with the occurrence of many lightning strikes. Flux precipitation, on the other hand, can be for example the shallow Winter rainfall (*stratiform* rain), but also the Fall heavy precipitation, which is associated with strong southerly wind ("Scirocco"). Note that these two classes are not

always mutually exclusive, since there can be some event producing heavy rainfall, which has strong southerly flux and some lightning strikes, as happens when small thunderstorms are embedded inside large precipitating structures. The basic idea of this simple two–parameter approach is to use two sounding–derived indices to describe the main trend of these two categories of rainfall.

The rain convective mechanism is then associated with the temperature difference between the Most Unstable Parcel lifted at 500 hPa and the corresponding environment. It is called DT500 and is similar to the classical Lifted Index. DT500 is a typical parameter to estimate the *convective instability*, as also shown by its ability to discriminate thundery 6 h periods from non–thundery periods, found by Manzato (2003)[6]. On the other hand, the rain flux mechanism is associated with the mean North–South component of the water vapour flux in the lowest 3 km of atmosphere: $\mathrm{VFlux} = \frac{1}{3000} \int_{z_{sfc}}^{z_{sfc}+3000} v(z) \cdot \rho_v(z)\,\mathrm{d}z$, see Manzato (2003) for details.

Figure 5 shows the annual cycle of these two indices, doing a 10–day moving average. Only the values derived from the 12 and 18 UTC soundings are used, because these are the periods with higher frequency of thunderstorms and rainfalls. The bold line shows the 10–day mean value of all the soundings of the Julian day, while the thin lines represent ± 1 standard errors (10–days moving average). Figure 5 a shows the annual cycle of DT500: it is possible to see how the minimum values (DT500 $< 0\,^{\circ}$C, meaning instability) are mainly measured during June, July and August, when there is the maximum frequency of the strongest thunderstorms. That means that the atmosphere convective instability is well associated to the thunderstorm intensity estimated by CALCA6h.

Figure 5 b shows the annual cycle of VFlux. In this case negative values mean winds blowing from the South. VFlux is much more scattered than DT500, because in general the wind fields are less smooth than the thermic ones. Nevertheless, it is possible to see two periods with on average strong southerly vapour flux: one from the end of April to the beginning of July (VFlux $\cong$ -8 $\mathrm{gs^{-1}m^{-2}}$) and the other – stronger – from mid September

[6] In that case the best discriminant value for thunderstorm occurrence was DT500 $< 1.4\,^{\circ}$C.

to late November (mean VFlux $\cong$ -10.5 $gs^{-1}m^{-2}$).

Figure 6 a shows the annual cycle of the relative humidity in the low levels (the lowest 250 hPa), called LRH. It is possible to see a gap of humidity between mid July and the end of August, while there is a peak at the beginning of October. Finally, figure 6 b shows the mean annual cycle of the Level of Free Convection (LFC), which is higher during Summer and lower in Fall. This parameter is evaluated only on the subset of the potentially unstable soundings.

Combining the two effects of humidity flux and potential instability one obtains figure 7, where a 30–day moving average is applied to smooth the strong variations of VFlux. This figure shows the main (heavily filtered) annual cycle[7] of the point [DT500, VFlux], and is comparable with the monthly histograms of figure 4. The mean values of DT500 and VFlux are used to divide the plane in quarters. On the top–right corner of figure 7 there are the Winter months, with low vapour flux and very stable soundings. On the bottom–right corner there are the Fall months, with mainly high vapour flux and quite stable soundings. Summer months are characterized by a low stability, which from July to mid August becomes mainly instability.

April, September and November are months with strong transitions. It is possible to see how the worst combination of strong VFlux and not sufficiently high DT500 can occur in September, when it is possible to have a concurrence of potential instability and strong flux. It is very interesting to note also that September has a mean LFC, derived from the Udine radiosounding, of about 2.1 km, while June has a mean value of 2.4 km (figure 6 b). The moist air is easier to lift than the drier air, because its density is lower. So, even if September has a lower potential instability than June, when there is strong moist flux it should be easier to realize that potential instability, lifting the moist air up to the – low – LFC. For example, Kerkmann (1996) suggests that the thunderstorm associated with heavy rainfall in September can be triggered by a *convergence line*, generated when the southerly Scirocco moist wind blows against the northern colder outflow coming from the

[7] This cycle diagram is similar to that firstly introduced by Brooks et al. 2006, this same issue.

mountains. That could explain why in September convective instability and strong flux are often combined together to produce heavy rain.

Between the end of June and the beginning of July it is also possible to have negative mean DT500 and quite large VFlux and that can produce very strong thunderstorms. From mid July to mid August there is a gap in VFlux. In that period the contribution to the total rain can be said to be mainly "convective" precipitation. Instead, the rain of October and November can be said to be mainly "flux" precipitation. During other periods of the year (for example May, June and September) it is very difficult to discriminate unambiguously between these two rainfall mechanisms.

6 Combining the two indices

It can be interesting to check the sensitivity of the maximum 6 h rain value to DT500 and VFlux. In figure 8 the plane DT500–VFlux is divided in a 12 x 12 grid, and in each box is shown the mean value of all the rainfalls, greater than 1 mm in 6 h, which fall in that bin. Differently than in the previous figures, here DT500 and VFlux are not *average* values and for this reason their scales are much larger then before (in this case outliers are not filtered out). The mean–rainfall value is represented in each box using a scale of six different blue colors.

If $|\mathrm{VFlux}| < 0.03\,\mathrm{kg\,s^{-1}m^{-2}}$ then the maximum rain is usually very low, at least if there is no very strong instability (i. e. if DT500 > -2 °C). Instead, if the southerly flux is very strong, then the maximum rain can be very high, even if the sounding is neutral (as happens when it is close to saturation). The red lines plotted in figure 8 represent a parameter obtained from the two previous indices and called "Buoyancy–Dynamic" index:

$$\mathrm{BuDyn} = \frac{\mathrm{DT500}}{200} + \mathrm{VFlux} \qquad [\mathit{dimensionless}]\,, \tag{3}$$

where 200 is a normalization coefficient, chosen to make the two indices more similar (VFlux is of the order of 10^{-2} $\mathrm{kg\,s^{-1}\,m^{-2}}$, while DT500 is of some °C). For example all the first five episodes listed in table 2 have BuDyn < -0.05 and two of them have BuDyn < -0.15.

The linear correlation between the maximum 6 h rain and VFlux (for the 3970 cases with more than 1 mm and no missing VFlux) gives a result of R = -0.32, while the same correlation done for BuDyn becomes R = -0.37 (p–value $< 2.2\,10^{-16}$), i. e. slightly better. That shows how difficult it is to forecast the maximum rain quantity well, even using observed data for doing short term forecast. To obtain larger correlation coefficients with the maximum rainfall one has to use more indices together, not just two, to take into account more aspects. That is done by the author (using neural network models) on a following article in this same issue.

7 Conclusions

The "6 h–period of the day" and the monthly distributions of thunderstorms and rainfalls in the FVG plain have been computed on the basis of the data collected during 10 years for thunderstorms and during 13 years for rainfall. Thunderstorms are more frequent in the FVG plain during afternoon and evening and from June to August. In particular, the strongest thunderstorms occurred more frequently in *July* and *August*, followed by September and June. It is also found that the strongest thunderstorm occurrence frequency can be described by the mean DT500 annual cycle, except for September, which has a frequency of strongest thunderstorms similar to June even if it has larger DT500 mean values (less instability). The strong thunderstorms of September are associated also to a decrease of the mean LFC height and to an increase of the water vapour flux, which can facilitate the thunderstorm trigger.

The most frequent rainfalls occur in two periods: during late Spring (April to June) and around October. Nevertheless, the heaviest rainfalls (meaning MaxRain > 39 mm in 6 h) occur more frequently during *September*, *October*, *August*, July, November, June, May and April, respectively. While the strongest rainfalls of July and August are mainly due to a great convective instability alone, in September and October the – lower – instability is often associated with a strong vapour flux in the lowest 3 km, which contributes to increasing the maximum rain quantity.

From the end of April to mid September the mean VFlux is generally not too strong, so the convective instability plays a crucial role. From the end of September to mid November VFlux is mainly dominating. In other periods it is not easy to discriminate between these two different mechanisms. In particular, the maximum of flash-flood frequency during September is probably due to a *concurrence of effects*.

A new index, BuDyn, based on DT500 (instability) and VFlux (wind and humidity) has been tested for forecasting the maximum rainfall amount accumulated in 6 h in the FVG plain. The correlation found (R = -0.37) is statistically significant, but quite low if used operationally.

Acknowledgments

Marcellino Salvador and Sergio Nordio (forecasters of OSMER–ARPA FVG, I) have drawn the author's attention to the importance of SST. Prof. Daniela Řezáčová (Institute of Atmospheric Physics, Prague, CZ) and the other anonymous reviewer provided precious suggestions. Gianbattista Toller (Istituto Agrario di San Michele all'Adige, Trento, I) gave helpful suggestions about the use of the R software. The author wants to thank his wife and dr Griffith Morgan for the English improvement and the encouragement. Last but not least, he thanks the "GNU generation" for having provided such good – and free! – tools as R, Python, LaTeX, Emacs, as well as Linux itself.

References

Brooks, H. E., Anderson, A. R., Riemann, K., Ebbers, I., Flachs, H., 2006. Climatological aspects of convective parameters from the NCAR/NCEP reanalysis. *Atmos. Res.* (this issue).

Buzzi, A., Morgan, G., Tibaldi, S., 1991. MATREP – a multi–agency experiment in co–ordinating measurements of thunderstorm phenomena in the Po Valley of northern Italy. *Bull. WMO* **40**, 321–327.

Cacciamani, C., Battaglia, F., Patruno, P., Pomi, L., Selvini, A., Tibaldi, S., 1995. A climatological study of thunderstorm activity in the Po Valley. *Theor. Appl. Climatol.* **50**, 185–203.

Ceschia, M., Micheletti, S., Carniel, R., 1991. Rainfall over Friuli–Venezia Giulia: High Amounts and Strong Geographical Gradients. *Theor. Appl. Climatol.* **43**, 175–180.

Cicogna, A., Nordio, S., Micheletti, S., 2000. Diurnal Course of Rainfall in the Plain of Friuli–Venezia Giulia: Evaluation of Hourly Measurements. *Theor. Appl. Climatol.* **65**, 175–180.

Frei, C., Schär, C., 1998. A precipitation climatology of the Alps from high-resolution rain-gauge observations. *Int. J. Climatol.* **18**, 873–900.

Gentilli, J., 1964. *Il Friuli – I climi*. Camera di Commercio, Industria e Agricoltura di Udine, 595 pp..

Giaiotti, D., Gianesini, E., Stel, F., 2001. Heuristic considerations pertaining to hailstone size distributions in the plain of Friuli Venezia Giulia. *Atmos. Res.* **57**, 269–288.

———, Stel, F., 2006. The effects of environmental water vapor on hailstone size distributions. *Atmos. Res.*, In Press, Corrected Proof, Available online 6 March 2006, doi:10.1016/j.atmosres.2006.02.002

Kerkmann, J. K. H., 1996. Case studies of severe convective storms in the Friuli area. *Map Newsletter* **4**, MeteoSwiss, 6–12. [available on line at http://www.map.ethz.ch/newsletter4.htm]

Manzato, A., 2003. A climatology of instability indices derived from Friuli Venezia Giulia soundings, using three different methods. *Atmos. Res.* **67–68**, 417–454.

Marullo, S., Guarracino, M., 2003. L'anomalia termica del 2003 nel Mar Mediterraneo osservata da satellite. *Energia, ambiente e innovazione* **49**, 48–53

Nappi, D., Bruno, F., 2004. Indici per la previsione dei temporali. *Rivista di Meteorologia Aeronautica* **1/2004**, 7–26.

Nelson, S. P., 1983: The Influence of Storm Flow Structure on Hail Growth. *J. Atmos. Sci.* **40**, 277–279.

Pradier, S., Chong, M., Roux, F., 2002. Radar observations and numerical modeling of a precipitating line during MAP IOP 5. *Mon. Wea. Rev.* **130**, 2533–2553.

Schulz, W., Cummins, K., Diendorfer, G., Dorninger. M., 2005. Cloud-to-ground lightning in Austria: A 10-year study using data from a lightning location system. *J. Geophys. Res.* **110**.

Vrhovec, T., Rakovec, J., Gregorič, G., 2004. Mesoscale diagnostics of prefrontal and frontal precipitation in the Southeast Alps during MAP IOP 5. *Metereol. Atmos. Phys.* **86**, 15–29.

Weickmann, H. K., 1953. Observational data on the formation of precipitation in cumulonimbus clouds, *Thunderstorm Electricity*, University of Chicago Press, 66–138.

TABLE CAPTIONS

Table 1. The six strongest thunderstorm 6 h periods, as measured by CALCA6h, occurring in the FVG plain during the years 1995–2004.

Table 2. The nine heaviest 6 h flash–floods occurring in the FVG plain during the years 1992–2004.

FIGURE CAPTIONS

figure 1. *The Friuli Venezia Giulia region with the four sub–areas (rectangles forming the target area) and the OSMER–ARPA surface station locations. In the middle of the region, near Udine, there is the 16044 sounding station, managed by the Italian Aereonautica Militare. Orographic elevation is in meters m. s. l. (adapted from Manzato 2003).*

figure 2. 2 a: *The thunderstorm occurrence frequency during the 6–h periods of the day, stratified in three classes of intensity, using the 90 % (dark columns) and 10 % (light columns) percentiles of CALCA6h.*
2 b: *The maximum rain occurrence frequency during 6–h periods of the day, stratified in three classes of intensity, using the 95 % (dark columns) and 41 % (light columns) percentiles of MaxRain.*

figure 3. 3 a: *The CALCA6h distribution for all the 1505 cases with at least three lightning strikes during the 6 h of each period, from April to November of years 1995-2004. Dotted lines show the 10 % (0.33) and 90 % (0.79) percentiles.*
3 b: *The maximum rain measured by any of the 15 OSMER–ARPA ground stations for all the 4147 6 h periods with at least 1 mm of accumulated rainfall, during the years 1992–2002. The number of cases in each 5 mm bin is shown on a logarithmic scale. The fitting line is given by equation 2. Dotted lines show the 41 % (5 mm) and 95 % (39 mm) percentiles.*

figure 4. 4 a: *The monthly thunderstorm occurrence frequency, stratified as in figure 2 a. Note how September has a lower frequency of "all" thunderstorms but a similar frequency of "strong" thunderstorms, when compared with June.*
4 b: *The monthly maximum rain occurrence frequency, stratified as in figure 2 b. Note how the maximum of frequency for "all" rainfall occurred in June, while that for the "strong" rainfalls occurred in September. The continuous line with dots shows the mean monthly SST measured by the OSMER–ARPA "Trieste Molo" station during the year 1995–2004 (Upper Adriatic). Instead the dashed line with dots shows the monthly SST on the mean Mediterranean Sea during the years 1985–2002, adapted from figure 6 of Marullo and Guarracino (2003).*

figure 5. 5 a: *The annual cycle of the 10–day moving average DT500 index, computed using the 12 and 18 UTC Udine soundings of each Julian day, for all the years 1992–2004. The thin lines show* ± 1 *standard error, i. e.* $\frac{\sigma}{\sqrt{N}}$.
5 b: *Same as 5 a, but for the VFlux index. A negative value means flux from the South. This index has more high–frequency variations than DT500.*

figure 6. 6 a: *Same as 5 a, but for the relative humidity in the lowest 250 hPa (LRH). Note the gap from mid July to August and the peak at the beginning of October.*
6 b: *Same as 5 a, but for the Level of Free Convection height, which is higher in Summer and lower in Fall.*

figure 7. *The annual cycle of the 30-day moving average DT500 vs. the 30-day moving average VFlux. On the top–right corner are the months with low North–South water vapour flux and high stability, while the left–bottom corner means soundings close to instability and with high VFlux. The labels are written near the middle of the month points. The two gray lines used to divide in quarters correspond to the mean values of the DT500 and VFlux. Only the 12 and 18 UTC soundings have been used.*

figure 8. *A "density plot" of the main maximum–rainfall as a function of DT500 and VFlux (not averaged). The 12x12 grid uses six different blue colors to show the mean rainfall of each box. The legend shows the MaxRain interval associated to each color, measured in mm. The red lines show isolines of BuDyn, as defined by equation 3.*

TABLES

Table 1.

Year	**Month**	**Day**	**Hours**	**CALCA6h**	**num_light** [number]	**rain** [mm]	**wind** [m/s]	**DT500** [C]
2000	9	16	17-23	0.996	3872	331	13.4	-3.6
1996	6	19	17-23	0.992	1858	371	16.2	-4.8
2002	8	1	17-23	0.972	2428	302	13.5	-5.2
2000	6	24	23-05	0.967	1587	142	22.8	-3.0
2002	8	6	23-05	0.957	2629	181	14.4	*miss*
1997	9	13	17-23	0.955	2096	326	11.8	-2.0

Table 2.

Year	**Month**	**Day**	**Hours**	**Station**	**Rain6h** [mm]	**DT500** [C]	**VFlux** [$\mathrm{kg\,s^{-1}m^{-2}}$]
1997	9	13	17-23	Capriva GO	184	-2.0	-0.069
1998	10	6	17-23	Faedis UD	161	-1.3	-0.152
1995	9	19	11-17	Cervignano UD	132	-0.2	-0.065
1998	9	12	11-17	Gradisca GO	114	+0.7	-0.060
1998	9	12	23-05	Fagagna UD	110	-4.1	-0.130
1992	9	28	23-05	Palazzolo UD	110	+0.7	-0.030
1995	6	11	23-05	Fossalon GO	109	-0.1	-0.046
2004	10	31	05-11	Brugnera PN	104	*miss*	-0.013
2002	9	19	17-23	Gradisca GO	101	-2.0	-0.018

FIGURES

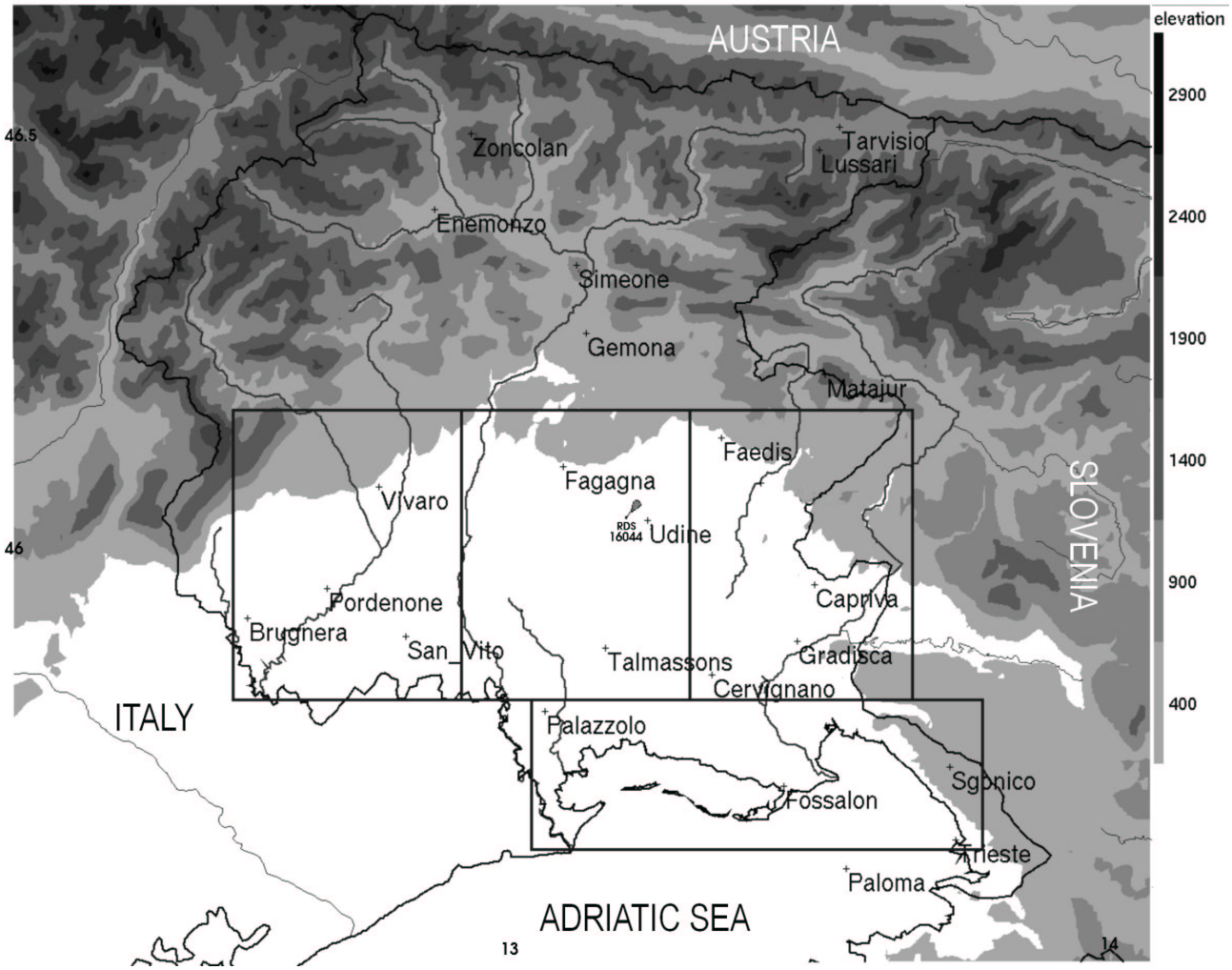

fig. 1

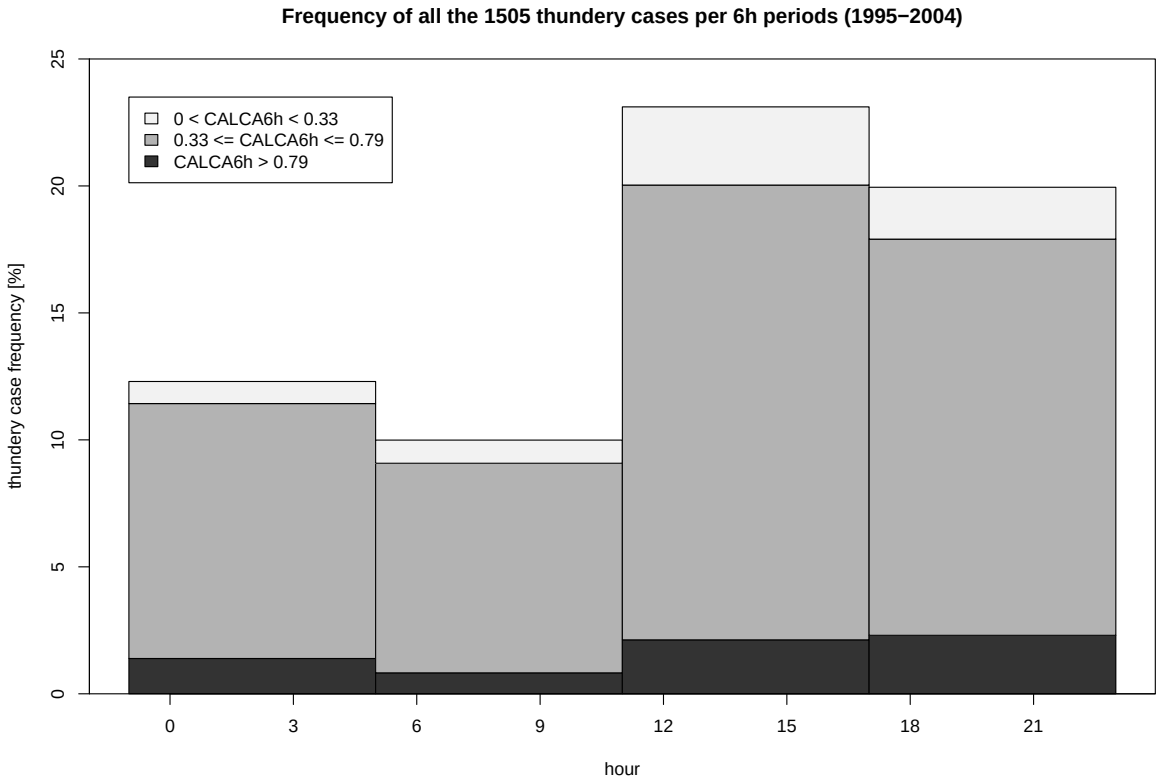
Frequency of all the 1505 thundery cases per 6h periods (1995−2004)
0 < CALCA6h < 0.33
0.33 <= CALCA6h <= 0.79
CALCA6h > 0.79
thundery case frequency [%]
0
5
10
15
20
25
0
3
6
9
12
15
18
21
hour

fig. 2a

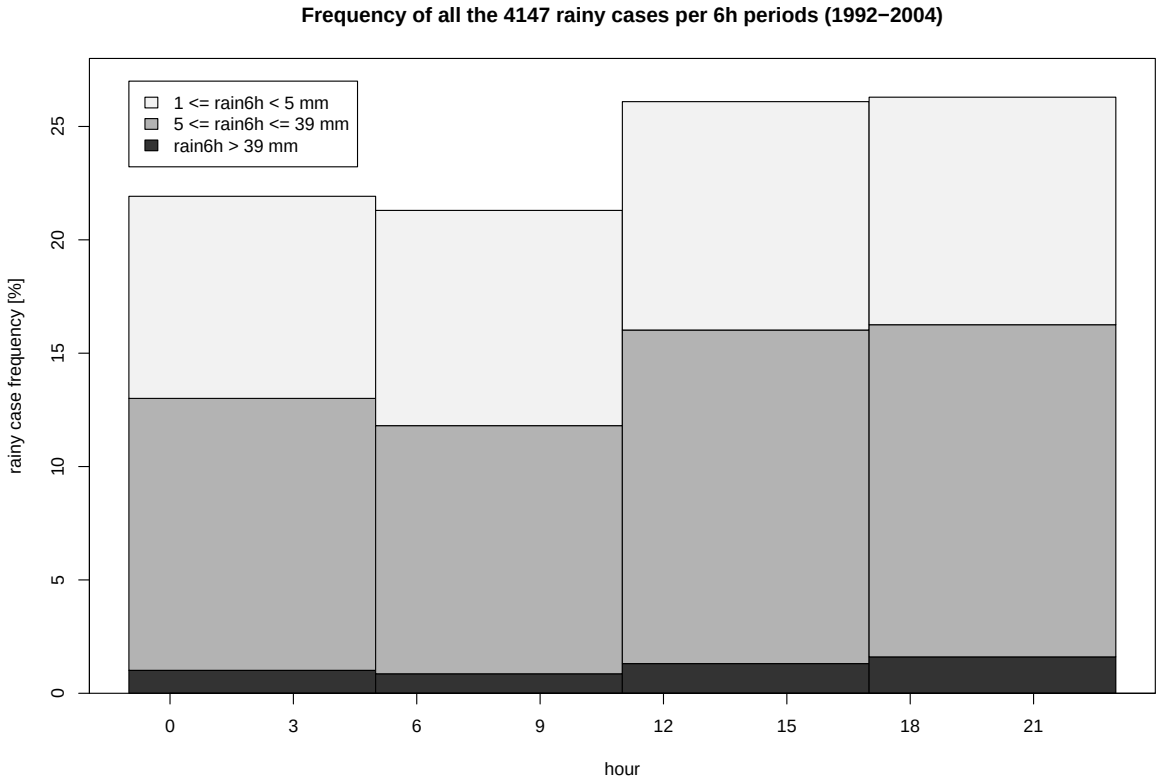
Frequency of all the 4147 rainy cases per 6h periods (1992−2004)
1 <= rain6h < 5 mm
5 <= rain6h <= 39 mm
rain6h > 39 mm
rainy case frequency [%]
0
5
10
15
20
25
0
3
6
9
12
15
18
21
hour

fig. 2b

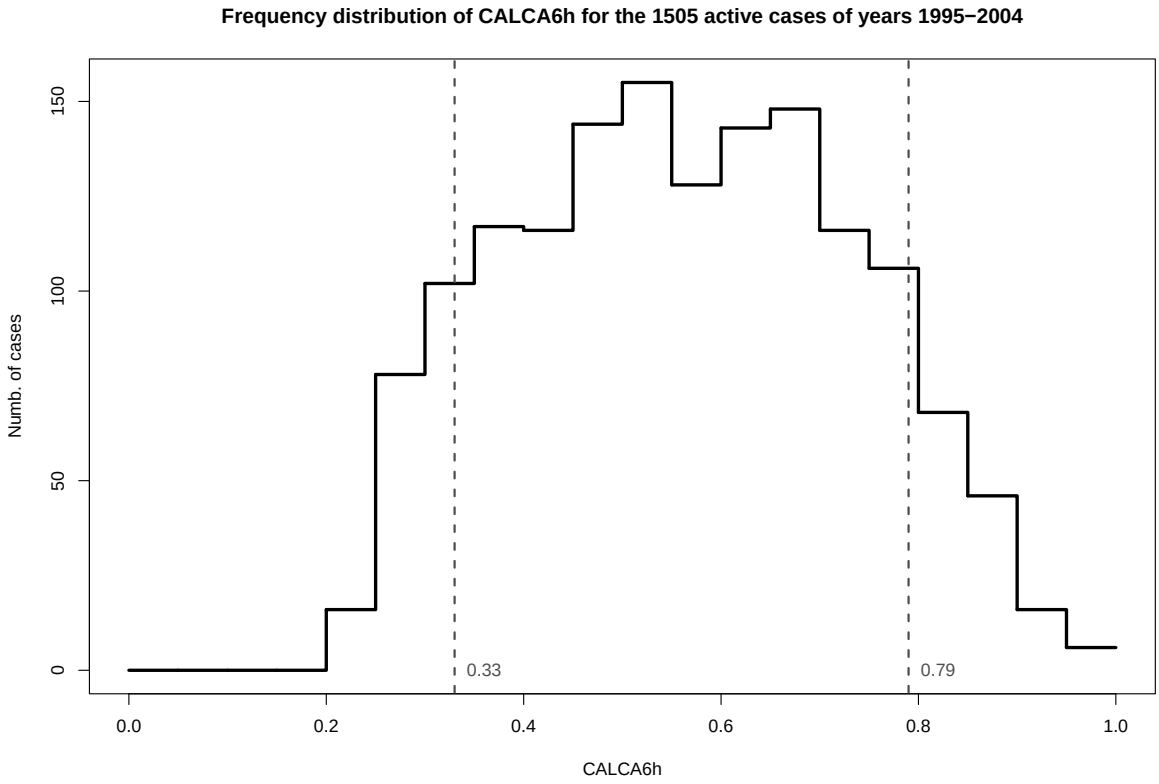
Frequency distribution of CALCA6h for the 1505 active cases of years 1995−2004
Numb. of cases
0
50
100
150
0.33
0.79
0.0
0.2
0.4
0.6
0.8
1.0
CALCA6h

fig. 3a

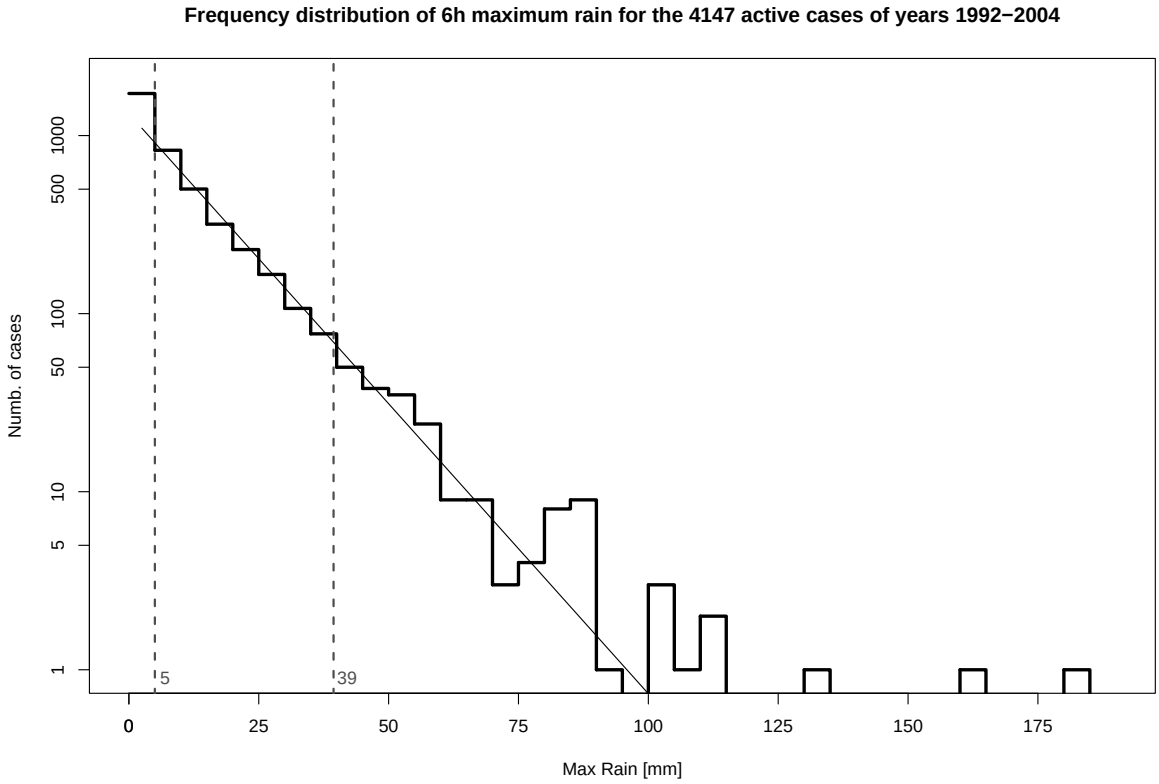
Frequency distribution of 6h maximum rain for the 4147 active cases of years 1992−2004
Numb. of cases
1
5
10
50
100
500
1000
5
39
0
25
50
75
100
125
150
175
Max Rain [mm]

fig. 3b

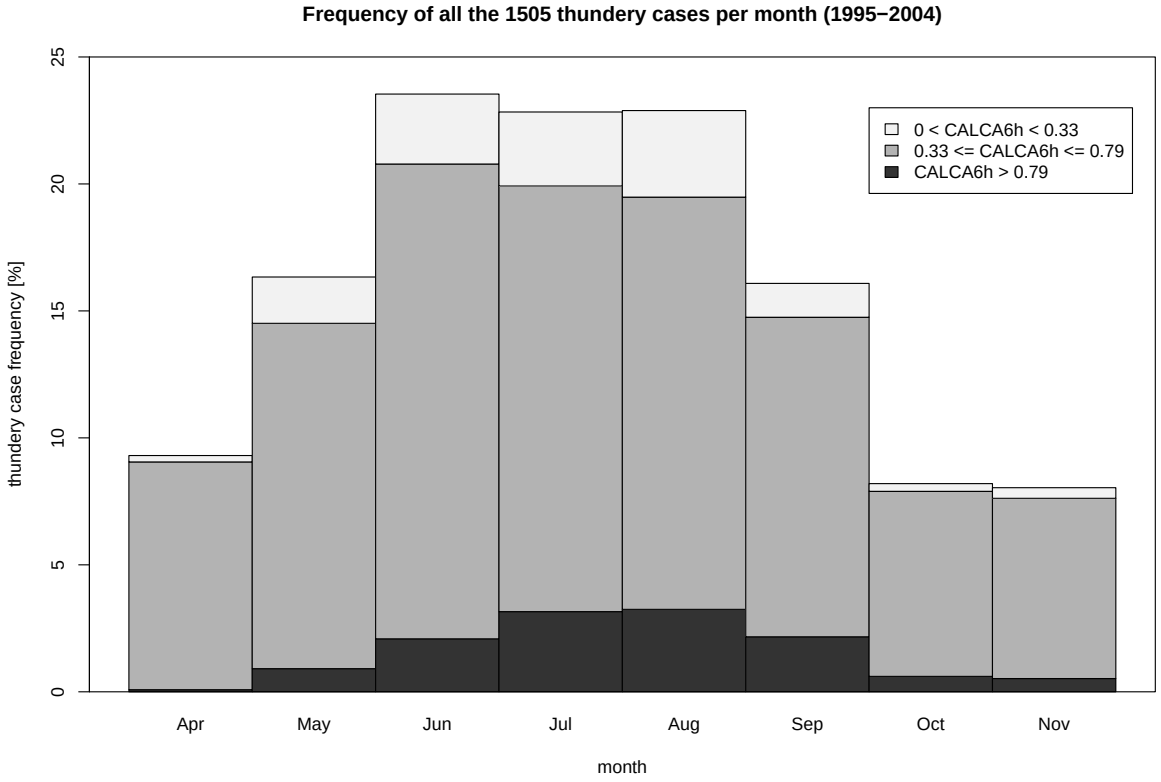
Frequency of all the 1505 thundery cases per month (1995−2004)
thundery case frequency [%]
0 < CALCA6h < 0.33
0.33 <= CALCA6h <= 0.79
CALCA6h > 0.79
Apr
May
Jun
Jul
Aug
Sep
Oct
Nov
month

fig. 4a

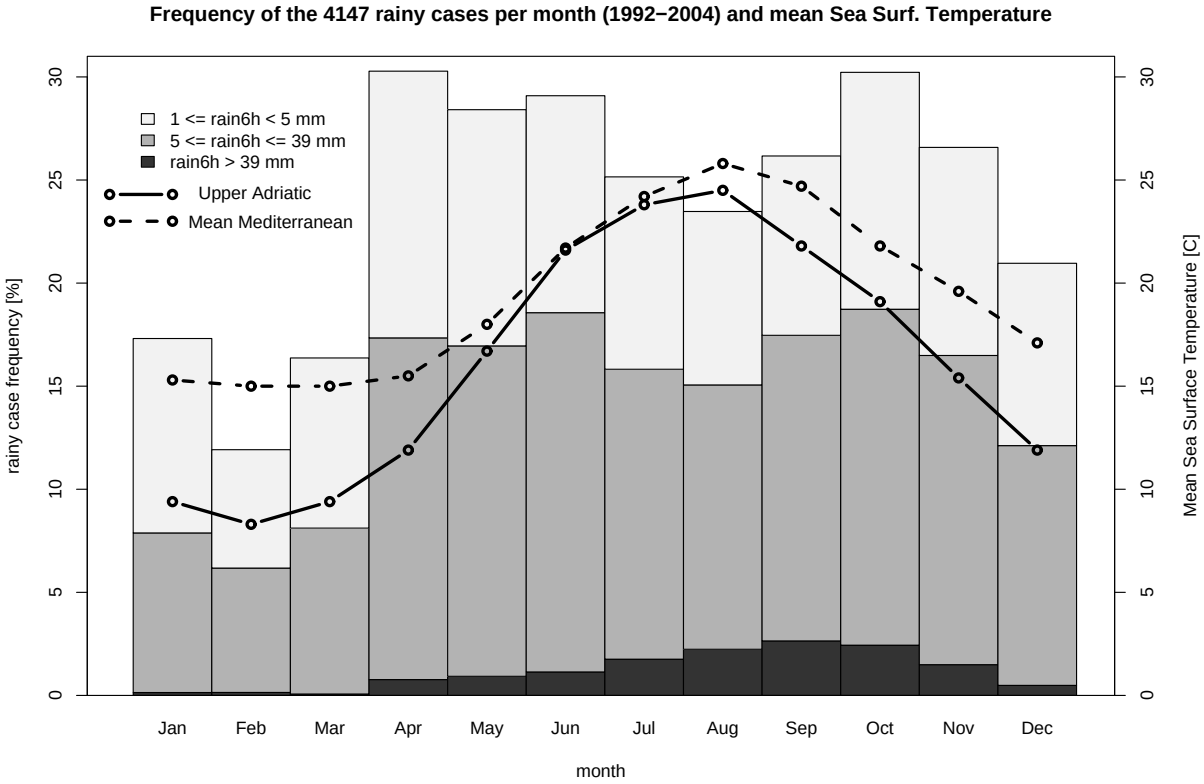
Frequency of the 4147 rainy cases per month (1992−2004) and mean Sea Surf. Temperature
rainy case frequency [%]
Mean Sea Surface Temperature [C]
1 <= rain6h < 5 mm
5 <= rain6h <= 39 mm
rain6h > 39 mm
Upper Adriatic
Mean Mediterranean
Jan
Feb
Mar
Apr
May
Jun
Jul
Aug
Sep
Oct
Nov
Dec
month

fig. 4b

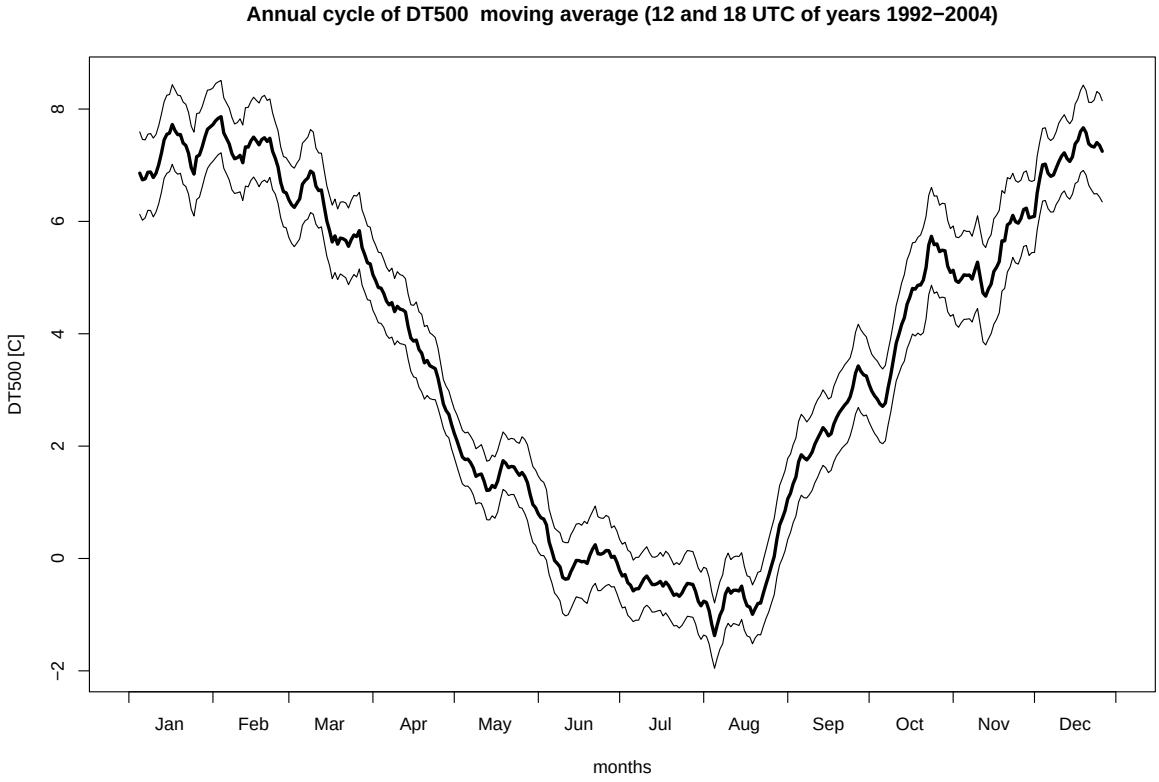
Annual cycle of DT500 moving average (12 and 18 UTC of years 1992−2004)
DT500 [C]
8
6
4
2
0
−2
Jan
Feb
Mar
Apr
May
Jun
Jul
Aug
Sep
Oct
Nov
Dec
months

fig. 5a

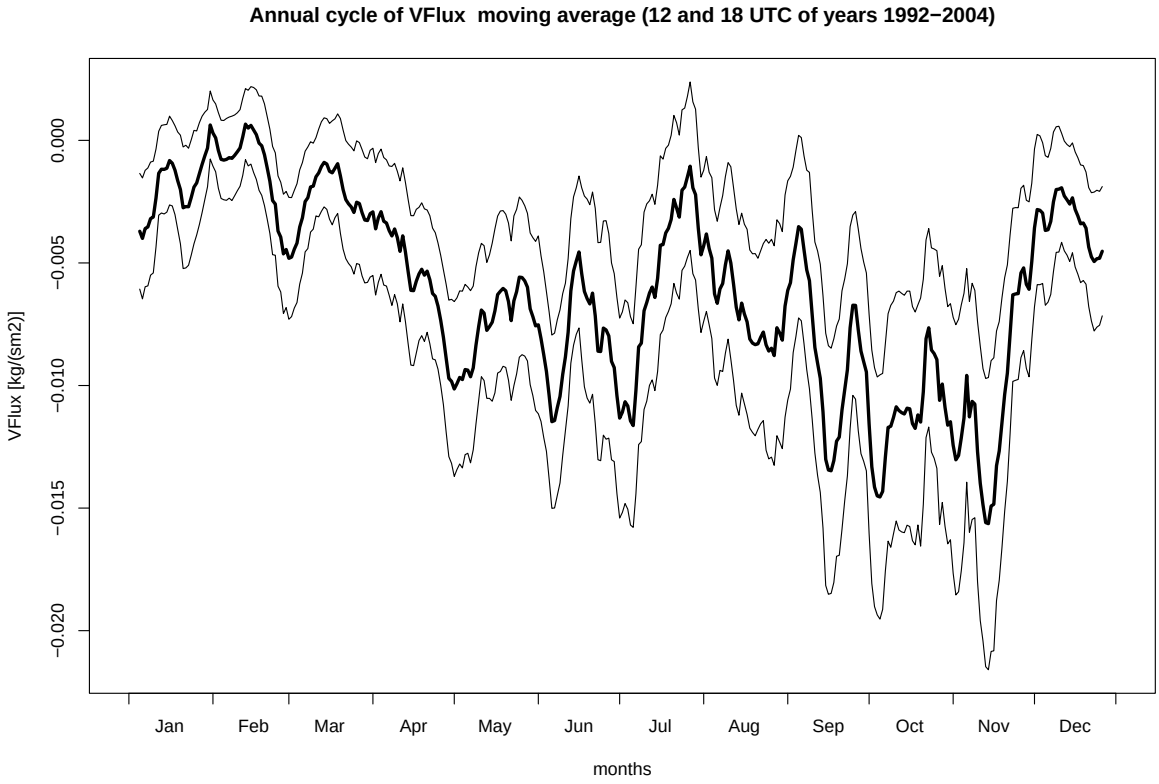
Annual cycle of VFlux moving average (12 and 18 UTC of years 1992−2004)
VFlux [kg/(sm2)]
0.000
−0.005
−0.010
−0.015
−0.020
Jan
Feb
Mar
Apr
May
Jun
Jul
Aug
Sep
Oct
Nov
Dec
months

fig. 5b

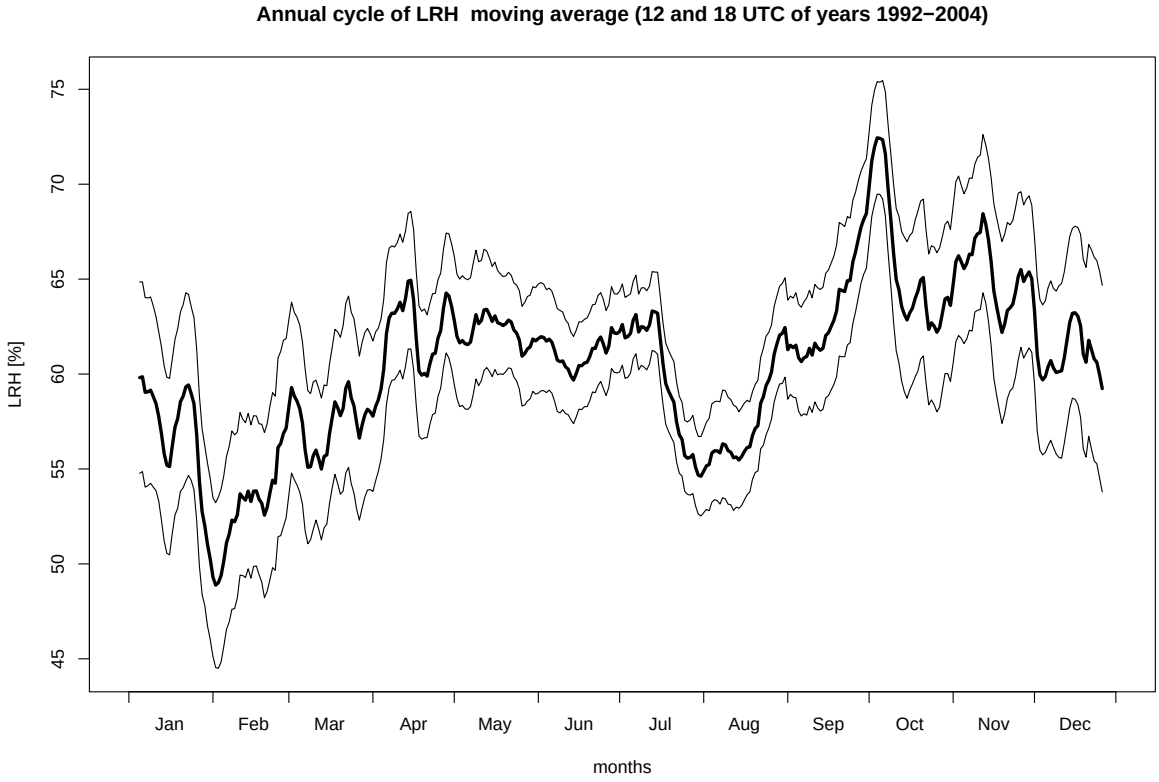
Annual cycle of LRH moving average (12 and 18 UTC of years 1992−2004)
LRH [%]
45
50
55
60
65
70
75
Jan
Feb
Mar
Apr
May
Jun
Jul
Aug
Sep
Oct
Nov
Dec
months

fig. 6a

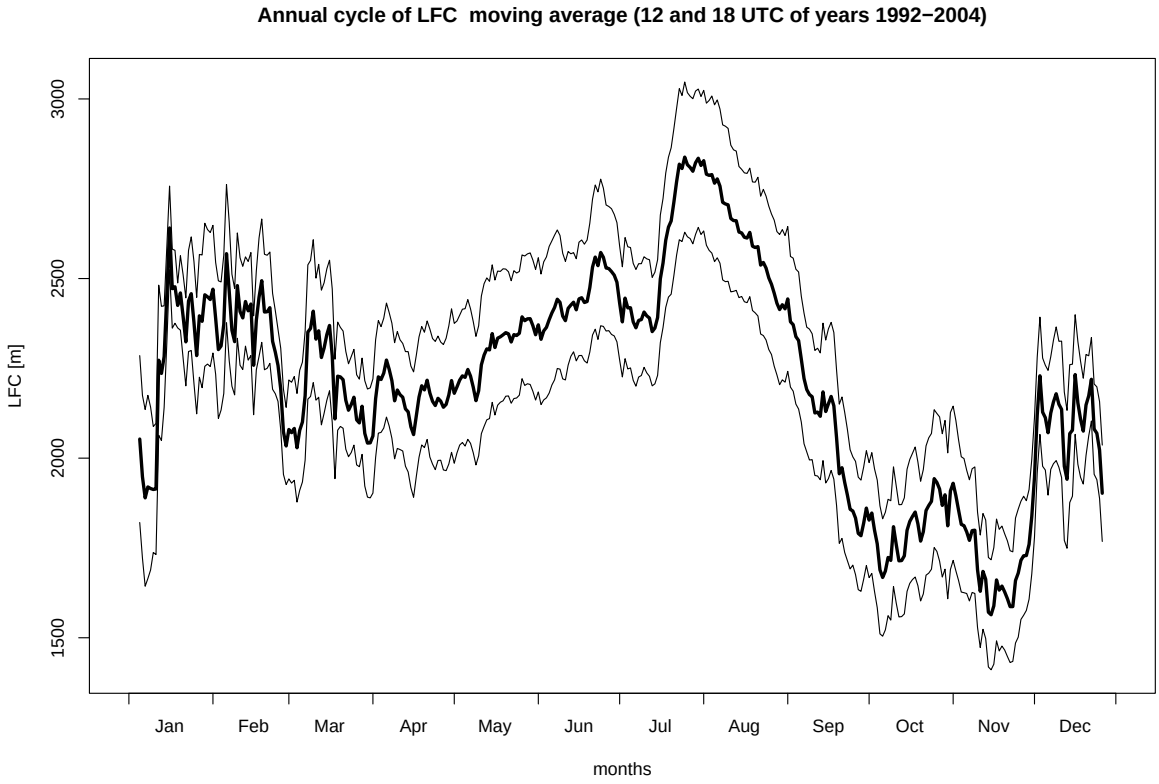
Annual cycle of LFC moving average (12 and 18 UTC of years 1992−2004)
LFC [m]
1500
2000
2500
3000
Jan
Feb
Mar
Apr
May
Jun
Jul
Aug
Sep
Oct
Nov
Dec
months

fig. 6b

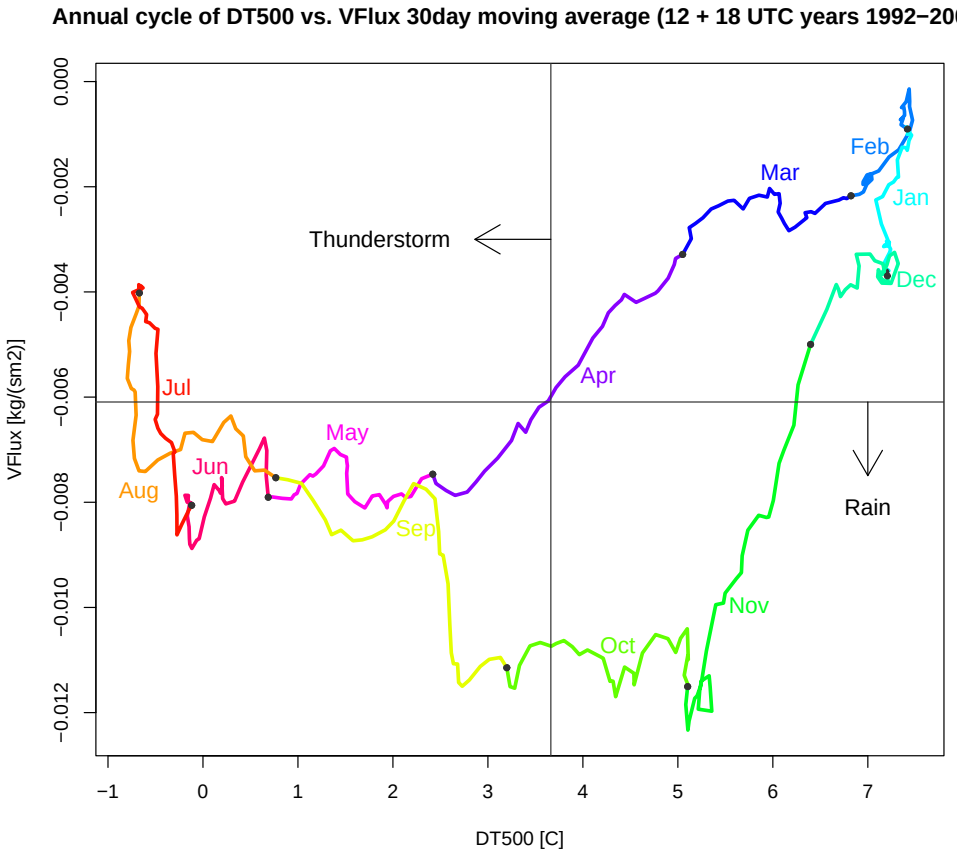
Annual cycle of DT500 vs. VFlux 30day moving average (12 + 18 UTC years 1992−2004)
VFlux [kg/(sm2)]
0.000
−0.002
−0.004
−0.006
−0.008
−0.010
−0.012
DT500 [C]
−1
0
1
2
3
4
5
6
7
Thunderstorm
Rain
Jan
Feb
Mar
Apr
May
Jun
Jul
Aug
Sep
Oct
Nov
Dec

fig. 7

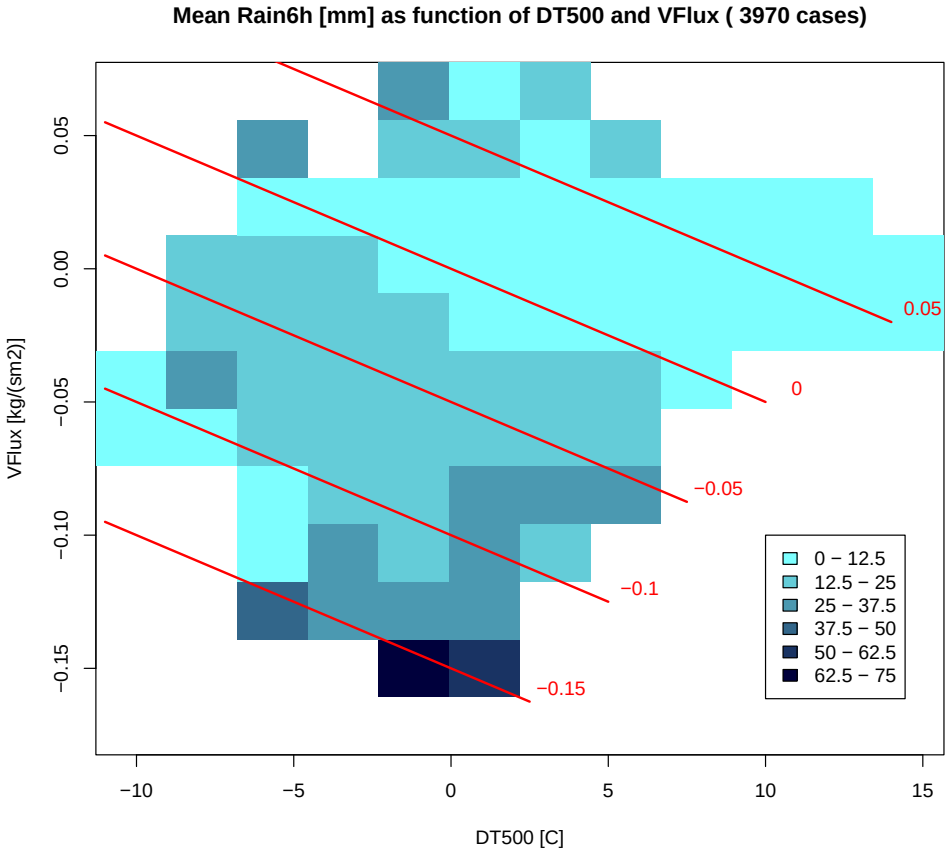
Mean Rain6h [mm] as function of DT500 and VFlux (3970 cases)
VFlux [kg/(sm2)]
0.05
0.00
−0.05
−0.10
−0.15
DT500 [C]
−10
−5
0
5
10
15
0.05
0
−0.05
−0.1
−0.15
0 − 12.5
12.5 − 25
25 − 37.5
37.5 − 50
50 − 62.5
62.5 − 75

fig. 8